Seasonal and Spatial Variation of Radiative Effects of Anthropogenic Sulfate Aerosol

Qian Yun (钱 云), *Wang Hongqi* (汪宏七)
Fu Congbin (符淙斌), *Wang Zifa* (王自发)
START Regional Center for TEA, Institute of Atmospheric Physics, Chinese Academy of Sciences, Beijing 100029
Received March 17, 1997; revised March 13, 1998

ABSTRACT

On the basis of the emission data of the industrial sulphur dioxide (SO_2) and observed climate fields over East Asia, the distribution of anthropogenic sulfate aerosol(SO_4^{2-}) with seasonal variation in the troposphere is simulated and analyzed by a regional sulfur transport model, and the direct radiative effects of SO_4^{2-} under different weather conditions are also calculated using the discrete ordinate method. The results show that the concentration of SO_4^{2-} has significant seasonal and spatial variations resulting from the effects of SO_2 emission source and precipitation and wind fields. Both the concentration of SO_2 and its radiative forcing have the largest values in October and the lowest in July. SO_4^{2-} causes the decrease of the radiation flux absorbed by earth-atmosphere and the cooling of air temperature by scattering more solar radiation back into space. Besides, the radiative and climatic effects of SO_4^{2-} are related to the types and height and optical thickness, etc., of the clouds.

Key words: Sulfate aerosol(SO_4^{2-}), Radiative effects, Seasonal and spatial variations

I. INTRODUCTION

Analysis of observed climate data revealed two remarkable facts: 1)Earth has been getting warmer and warmer since the beginning of industrialization while the daily range of air temperature is decreasing; 2) The warming rate in the Northern Hemisphere has been decreasing since 1940's (Danny, 1995). It's inferred that the forementioned changes are possibly due to the ever increasing human activities. The industrialization causes more and more consumption of mineral fuel, which results in, on the one hand, the larger CO_2 concentration and the stronger green-house effects, on the other hand, the more SO_2 emitted into air. As a result, increased sulfate aerosol(SO_4^{2-}) particles due to SO_2 emission may reduce the solar radiation absorbed by the earth-atmosphere system through reflecting more radiation back into space. Moreover (Charlson, 1991a), SO_4^{2-} can act as cloud condensation nuclei (CCN) and thus change the optical characteristics and life time of clouds, then, as so-called indirect forcing it causes the variation in the energy and radiation balance of earth-atmosphere and leads to the climate change (Charlson, 1991b).

Because of the specific optical nature of the SO_4^{2-}, its radiative effects present the following three characters which are different from CO_2's: the first is that the variability is large, including not only the diurnal and synoptic scale variation, but also the seasonal variation; the second is that SO_4^{2-} mainly influences the solar radiation, which implies the effects of sulfate are significant during daytime; the third is that the climatic effects of SO_4^{2-} are regional due

to its regional distribution (Qian and Fu, 1997).

The observation shows that East Asia has become the region where both the increment of SO_2 emission sources and the concentration of SO_4^{2-} in air are the largest in the globe because of its rapid social and economic developments, and it has been paid more and more attentions by the governments and scientists in the world (IPCC, 1994). In this paper the seasonal and spatial distributions of anthropogenic sulfate aerosol in the troposphere are simulated and analyzed by the regional sulfur deposition and transport model, and the radiative effects under the conditions of clear and cloudy sky are calculated using the discrete ordinate method. The research results will not only improve our basic understanding on radiative effects and characters of SO_4^{2-} under different weather backgrounds, but also provide foundation for comparison with parameterization schemes of SO_4^{2-} in complicated climate models.

II. SPATIAL DISTRIBUTION OF SO_4^{2-} IN DIFFERENT SEASONS

1. *Introduction of Chemical Transport Model*

A three-dimensional regional Eulerian model for sulfur deposition and transport is used to simulate the distribution of SO_2 and SO_4^{2-} (Huang et al., 1996). The equation of the model describes emission, transport, diffusion, gas-phase and aqueous-phase chemical process, dry deposition, rainout and washout of sulfur. The effects of temperature, humidity, light intensity, cloud and fog coverage and pollutant concentration on the oxidant rate of SO_2 are considered. The model uses a horizontal grid with $1^\circ \times 1^\circ$ resolution covering East Asia from 16°N to 50°N, and 98°E to 146°E. The vertical extending consists of eight layers from the surface to the tropopause along a sigma coordinate. It's supposed that the surface is an absorbed boundary while the top boundary a closed one. The lateral boundary condition is assumed that pollutants can only transport out of the domain but not into. Climatic datasets, such as wind, geopotential height, temperature, relative humidity, are obtained from ECMWF (Europe Center for Middle-range Weather Forecasts) and the rainfall datasets are interposed by observed data from the Meteorological Agency of China. The emission inventory for SO_2 over the mainland of China comes from China Environmental Agency, and those of other regions are taken from Akimoto (1994).

The scatterplot diagram of SO_4^{2-} concentration from the calculation and the observation in precipitation shows that the calculated results have a good agreement with the observed ones with a correlation coefficient of 0.80 and an average error of 23%.

2. *Vertical Distribution*

Vertical profile of area averaged SO_4^{2-} concentration (Fig. 1) shows SO_4^{2-} concentration decreases with the altitude in all seasons. But the variability under 1 km is relatively small, and the concentration at the top of boundary layer is even larger than that at surface, especially in July and October. The average concentrations in boundary layer are 0.30, 0.75, 2.2 and 1.8 mg m^{-3}, respectively in April, July, October and January. The concentrations in October and January are significantly larger than those in April and July. Generally, SO_4^{2-} is mainly distributed in lower layers of the troposphere below 2 km.

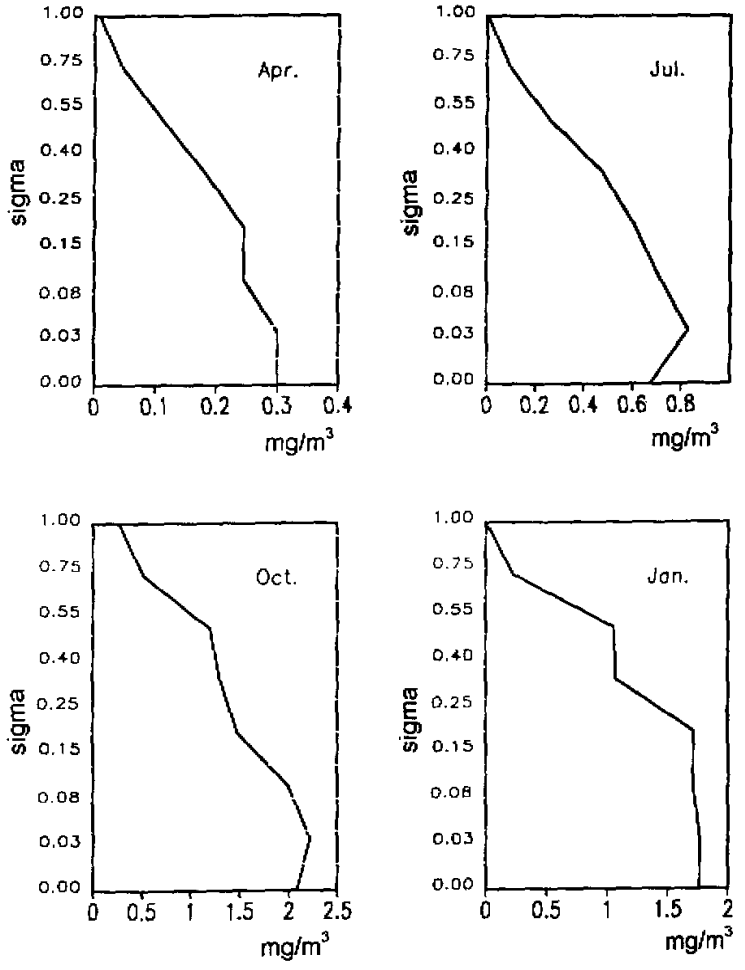

Fig. 1. Vertical profile of SO_4^{2-} concentration averaged in the model domain (mg m^{-3}).

3. *Horizontal Distribution*

Fig. 2 shows the SO_4^{2-} horizontal burden distribution integrated in the troposphere. It is found that SO_4^{2-} mainly locates in the central part of domain between 20°N and 40°N. There exists a tail shaped high value area in the western Pacific due to the westerly belt in upper layer. Over the land, there are three high value centers respectively in Southwest China, the middle and lower reaches of the Yangtze River and the lower reaches of the Yellow River. In January and July it is in Southwest China where the highest concentration of SO_4^{2-} occurs. In October it is in the middle and lower reaches of the Yangtze River being of the highest concentration.

The seasonal change of averaged concentration of SO_4^{2-} is significant and the highest

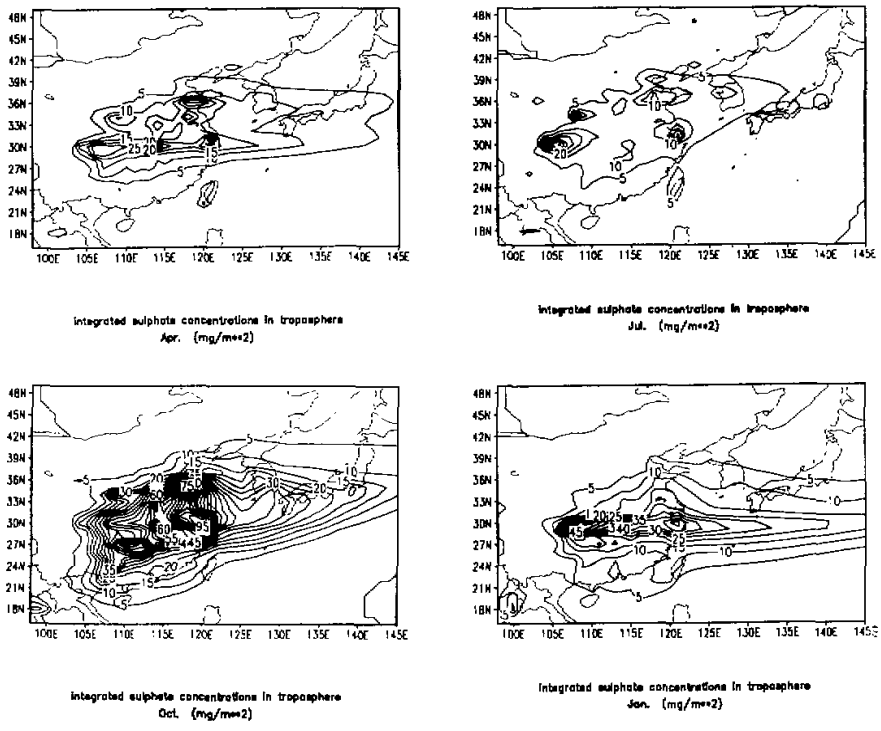

Fig. 2. Distribution of SO_4^{2-} burden integrated in the troposphere (mg m^{-2}).

average value occurs in October, then successively is in January, April and July. Mean SO_4^{2-} concentrations of domain are 5.7, 3.7, 11.1 and 2.5 mg m^{-2} in April, July, October and January. In some high value areas, mean SO_4^{2-} concentrations in the troposphere tend to be larger than over 10 mg m^{-2}. But the Northern Hemisphere and global averaged burden are 3.5 and 2.0 mg m^{-2} respectively according to Charlson (1992).

Simulated concentration distributions in different levels reveal that the SO_4^{2-} content in lower layers is relatively high and mainly locates over land, which consists with the distribution of SO_2 emission sources. With increasing altitude, the diffusion of SO_4^{2-} enhances, its distribution areas expand toward south and east and its concentration decreases simultaneously.

4. *Contributing Factors of Seasonal and Regional Variation*

From above analysis we find that SO_4^{2-} mainly distributes over land and lower reaches of westerly belt. The SO_4^{2-} concentration is larger in winter and fall than that in summer and spring. It results principally from following three factors:

(1) *Distribution of* SO_2 *emission source*

Anthropogenic SO_4^{2-} is mainly transformed from industrial SO_2 through chemical reaction under the conditions of either clear or cloudy sky. So the SO_4^{2-} distribution depends firstly on SO_2 concentration in the atmosphere that is mainly decided by local emission amount. Regional distribution of SO_2 shows that the areas with high value SO_2 locate over industrial regions, for example, Southwest China, the lower and middle reaches of the Yangtze River, the lower reaches of the Yellow River, Korean peninsula and Peking, Tianjin. Comparing with SO_4^{2-}, the pattern of SO_2 distribution is more close to that of the emission source, and the seasonal variation of SO_2 is the same as SO_4^{2-}'s.

(2) *Precipitation*

The seasonal variation of emission amount doesn't vary too much for a certain area, but the seasonal differences of SO_2 and SO_4^{2-} are obvious. It is primarily due to the wet removal of precipitation. The monthly precipitation distributions in four seasons are shown in Fig. 3. July is the rainy season in China, that is, the raining area stretches from South China to North China and the rainfall in most areas is above 100 mm / month. In July, SO_2 and SO_4^{2-} concentrations are lowest due to the strongest wet removal. In April the SO_2 and SO_4^{2-} concentrations are relatively small over South China because the precipitation is chiefly concentrated over there. In October it is clear over most parts of China, so the concentrations of

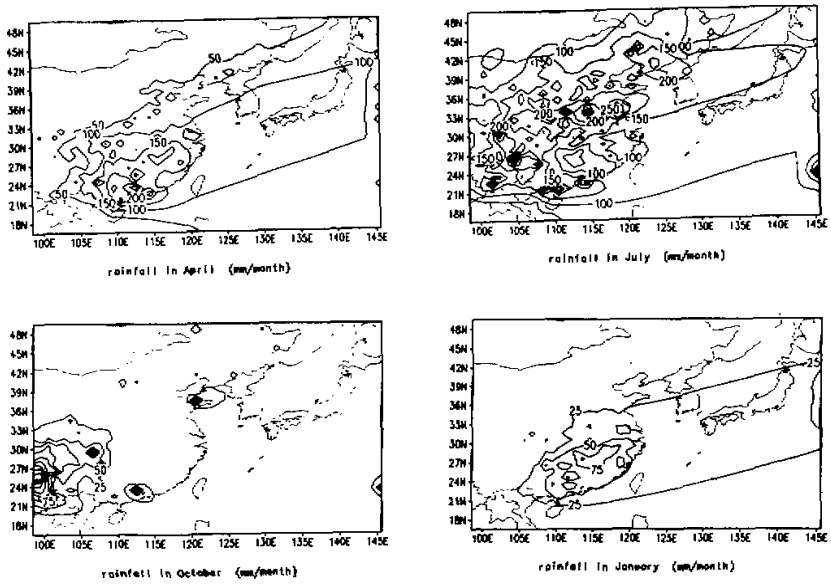

Fig. 3. Rainfall distribution in April, July, October and January (mm / Month).

SO_2 and SO_4^{2-} are the largest of the whole year. Of course air humidity would have influence on the transforming process of SO_2 to SO_4^{2-}.

(3) *Wind fields*

In addition to precipitation, general circulation is another important factor that can significantly affect the transport and distribution of SO_2 and SO_4^{2-}. Fig. 4 shows the wind fields at 850 hPa for four seasons. In July, the convergence of Indian and East Asian monsoons forms a strong souther in East and Middle China and a strong southwester in North China. This circulation pattern is beneficial to the diffusion and transport of sulfur in atmosphere. In April, southwesterly is prevailing in South China and so is westerly in North China. The wind is relatively weak in the middle of China. In January, because of the influence of Mongolia high, the northwesterly is prevailing to the south of the Yangtze River. From north to south the wind weakens with the decreased latitude. So the distribution of SO_4^{2-} moves southwards and has no obvious high value center in the lower reaches of the Yellow River. In October, the wind is relatively weak and a weak anticyclone appears over mainland. The atmospheric stratification at the same time is relatively stable. This circulation pattern is not advantageous to the diffusion and transport of SO_4^{2-}. It is one of the important reasons that leads to the high content of SO_4^{2-} in the atmosphere in October.

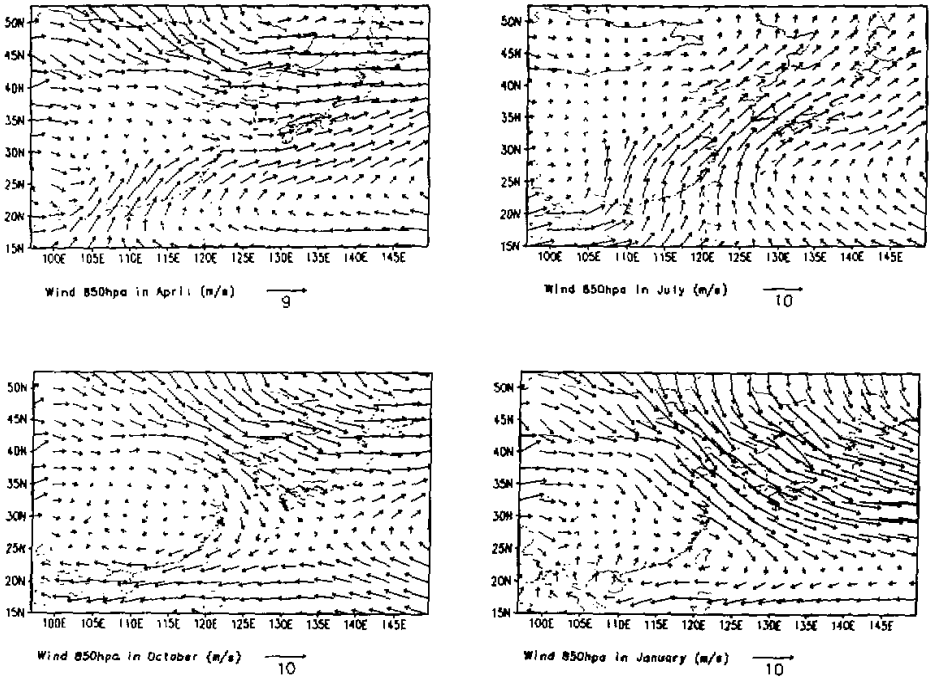

Fig. 4. Wind fields in 850 hPa in April, July, October and January.

III. THE RADIATIVE EFFECTS OF SO_4^{2-} IN CLEAR SKY

1. *Radiation Transfer Scheme and Calculation*

The δ-4 stream discrete ordinate method is used in the radiation transfer calculation(Stamnes et al.,1988). The range of wavelength considered is from 0.294 to 5 μm (2000–34000 cm^{-1}). The spectral resolutions are 20 cm^{-1} in the range of 2000–14000 cm^{-1}, 100 cm^{-1} in the 14000–20000 cm^{-1}, and 200 cm^{-1} in the 20000–34000 cm^{-1}, respectively. The effects of gaseous absorption, molecular Rayleigh scattering, aerosol absorption and scattering are included. The absorption gases concerned are H_2O, CO_2, O_3, CH_4, N_2O, CO and O_2. The effect of N_2 continuum absorption is also included. The gaseous absorption in each 20 cm^{-1} interval is regarded as monochromatic in the range of 0.294–0.56 μm, and in other wavelength ranges it is treated as pseudo-monochromatic by using exponential sum fitting. The effects of variations in the atmospheric temperature and pressure on the gas absorption are also taken into account in the calculation. The data of LOWTRAN7 are used (Kneizys et al., 1988). The profiles of the atmospheric temperature, pressure and component density for January and July come from midlatitude winter and summer atmospheric model; for April and October come from the 1976 U.S. standard atmospheric model. As for the aerosol profiles, the rural continental aerosol model with 23 km visibility is adopted in 0 – 2 km boundary layer; the background tropospheric aerosol model, background stratospheric aerosol model and upper atmospheric aerosol model are respectively used in the layers of 2–10 km, 10–30 km and above 30 km altitude. The extinction coefficient, single scattering albedo and asymmetric factor of the aerosol consisted of droplets with 75% H_2SO_4 are adopted as the corresponding optical parameters of SO_4^{2-} in the model (Deepak and Gerber, 1983). The surface albedo is adopted from seasonal average value given by Matthews(1983). The solar zenith angles used are the monthly daytime average values of solar zenith angle of January, April, July, and October, correspondingly.

The model atmosphere is divided into 14 layers in the vertical and there are 10 layers below 10 km. The height of every level (Z) varies with the height of topography (Z_S):

$$Z = Z_s + \sigma(10. - Z_s),$$

where σ is equal to 0.0, 0.03, 0.08, 0.15, 0.25, 0.40, 0.55, 0.75 and 1.0, respectively.

2. *The Vertical Variation of Heating Rate of Solar Radiation*

In the clear sky the heating rate of solar radiation increases with the altitude because of the absorption and scattering of tracer gases and aerosols in the atmosphere. The heating rate of solar radiation is the largest in July due to the strong radiant flux and high water vapor content in the atmosphere. It is on the contrary in January. The content of water vapor in atmosphere over South and East China in April is more abundant than that in October, so the averaged radiative heating rates in every layer in April are larger than those in October.

The introduction of SO_4^{2-} into calculation results in the radiative heating rates increasing in every layer, especially in the lower layers of the troposphere below 2 km. However, it is in the layers between 0.5 to 1.5 km instead of in the boundary layer that has the largest SO_4^{2-} concentration and the increase of heating rate of solar radiation is the largest. The SO_4^{2-} content in atmosphere is largest in October, so is its radiative heating rate. Through the analysis of the optical characteristics of SO_4^{2-} we can find that the absorption of SO_4^{2-} is

small, but the scattering is large at the short-wave lengths between 0.2 to 5.0 μm. The scattering increases the optical path of atmosphere which leads to an increment of radiative heating rate caused by other absorbing gases. Fig. 5 illustrates the vertical variations of solar radiative heating rates of four seasons over Southwest China. The vertical profiles over East China and whole domain have the similar characters with those of Southwest China.

3. *The Changes of Solar Radiation Flux on the Earth's Surface and at the Top of the Atmosphere*

The scattering of SO_4^{2-} results in the solar radiation arriving at earth's surface

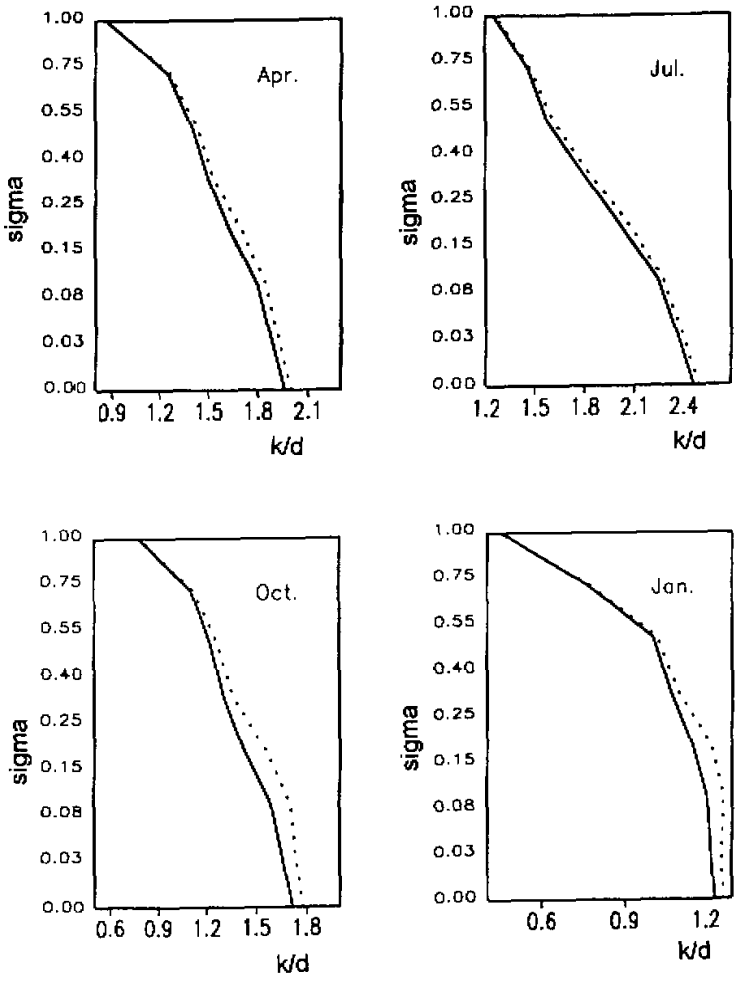

Fig. 5. Vertical profile of solar radiative heating rates of SO_4^{2-} in clear sky. Solid line: no SO_4^{2-}; Dashed line: SO_4^{2-} included (Unit: °C / d).

decreasing remarkably. In January and October, in high value region over the continent, the radiation flux decreases nearly 10 Wm^{-2}. In April and July, the decrease is more than 5 Wm^{-2}. The distribution of the radiation change coincides with that of SO_4^{2-} content. SO_4^{2-} causes solar radiative flux being reflected at the top of the atmosphere to increase, but the range of its variation is much less than that on the earth's surface. That is due to the reflection of the earth surface. The increment of reflected radiative flux represents the difference of albedo between the earth's surface and SO_4^{2-}.

Table 1. The Variations of the Solar Radiation Flux and the Radiative Heating Rates Caused by SO_4^{2-} under Clear Sky (Southwest China)

Season (Month)	SO_4^{2-} concentration ($mg\ m^{-2}$)	F_{SUR} ($W\ m^{-2}$)	F_{TOA} ($W\ m^{-2}$)	H_{BDY} ($^{\circ}C\ d^{-1}$)
Apr.	10.85	−3.10	0.56	0.038
Jul.	9.94	−2.82	0.49	0.031
Oct.	21.54	−5.86	1.21	0.060
Jan.	12.84	−3.10	0.76	0.029

Table 1 shows the variations of the solar radiation flux caused by SO_4^{2-} on the underlying surface (F_{SUR}) and at the top of the atmosphere(F_{TOA}) and the solar radiative heating rate (H_{BDY}) at the boundary layer (e.g. Southwest subregion). As SO_4^{2-} content in the atmosphere in October is much higher than that in July, the variation of solar radiation flux in October is as over twice as that in July. But neither the variation nor the seasonal difference of the radiative heating rate in the boundary layer is large. It implies that it is mainly through decreasing the solar radiation flux received by the earth's surface that SO_4^{2-} affects the heat exchange between the surface and the atmosphere and the variation of temperature.

IV. THE RADIATIVE EFFECT OF SO_4^{2-} IN THE CLOUDY ATMOSPHERE

Taking the Southwest subregion as an example, two groups of experiments are conducted to investigate the different radiative effects of SO_4^{2-} with the high cloud or low cloud. It is assumed that the low cloud is stratus(St), and the high cloud is altostratus(As), and the optical thickness of the high and the low cloud at 0.55 μm is 1 and 10, respectively.

1. *Low Cloud*

Supposing the low cloud is in the second layer of the model. As the result of strong absorption of the cloud droplets, the solar radiative heating rate increases by 4~ 5 times as that in clear sky. Owing to the thicker optical thickness of the low cloud, its absorption and reflection are stronger, and the solar radiative flux arriving the subcloud is on the obvious decrease, and the subcloud's radiative heating rate decreases rapidly. Because of the reflecting of the cloud and the change of the atmospheric optical path, the radiative heating rates in the layers above the cloud increase a little(See Fig. 6).

Table 2. The Radiative Heating Rates in Clear Sky and in the Cloudy Atmosphere (High Cloud and Low Cloud) and Its Variation Caused by SO_4^{2-} in above Different Conditions (Southwest China, Unit: °C / d)

Model layer	Clear sky		SO_4^{2-} heating rate		Low cloud		SO_4^{2-} heating rate		High cloud		SO_4^{2-} heating rate	
	Jan.	Jul.	Jan.	Jul.	Jan.	Jul.	Jan.	Jul.	Jan.	Jul.	Jan.	Jul.
1	1.24	2.47	0.03	0.03	0.16	0.49	−0.01	−0.01	1.01	2.28	−0.01	0.00
2	1.22	2.36	0.04	0.03	6.05	10.89	−0.32	−0.42	1.00	2.18	−0.01	0.00
3	1.21	2.25	0.06	0.03	1.71	3.28	0.07	0.04	0.99	2.08	0.00	0.00
4	1.15	2.03	0.07	0.05	1.46	2.58	0.07	0.06	0.95	1.87	0.00	0.01
5	1.07	1.80	0.03	0.04	1.25	2.07	0.03	0.04	0.88	1.65	0.00	0.01
6	1.00	1.58	0.02	0.04	1.11	1.72	0.02	0.04	0.82	1.47	0.00	0.01
7	0.77	1.46	0.01	0.02	0.84	1.54	0.00	0.02	1.31	2.07	0.01	0.01
8	0.45	1.25	0.00	0.01	0.46	1.25	0.00	0.01	0.50	1.30	0.00	0.01

The radiative heating rate decreases by about 0.3～0.4°C / d with the introduction of SO_4^{2-}. It shows that the scattering and reflecting of SO_4^{2-} are very strong. In the layers below the cloud, SO_4^{2-} causes decrease of about 0.01°C / d in the radiative heating rate, but above the cloud, it has reverse effect. From the higher altitude down to the lower altitude, the more it is near the cloud, the more the radiative heating rate increases. That is because the scattering effects of SO_4^{2-} increase, the atmospheric optical path gets longer, therefore the radiative heating rates increase above the cloud. The atmospheric optical path in the layers below the cloud seemingly increases because of the reflecting effects of SO_4^{2-} in the upper layers, the radiation flux which arrives that layer is abated, and the radiative heating rates are on the decrease, though the range of change is small(See Table 2).

SO_4^{2-} almost couldn't change the solar radiation flux which arrives the earth's surface when there are low clouds. But the upward solar radiation flux at the top of the atmosphere increases by about 0.05 Wm^{-2}. It shows that the solar radiation flux absorbed by the earth–atmosphere system decreases, but the order of its variation is only one–tenth as that in clear sky (See Table 3).

Table 3. The Variation of the Solar Radiation Flux on the Underlying Surface and at the Top of the Atmosphere Resulting from SO_4^{2-} in Cloudy Atmosphere (Southwest China)

	F_{SUR}(W m^{-2})		F_{TOA} (W m^{-2})	
	Jan.	Jul.	Jan.	Jul.
Low cloud	0.00	0.00	0.05	0.05
High cloud	−0.77	−1.15	0.55	0.46

2. *High Cloud*

Supposing the high cloud is in the 7th layer of the model. The calculated results show

that the solar radiative heating rate of this layer is larger than that in clear sky, but the increase range is much less than that in the condition of low-level cloud. Similar to the low-level cloud's radiative effects, the solar radiative heating rates get smaller in the layers below the cloud, and larger in the layers above the cloud, but it doesn't change much.

The radiative heating rates caused by SO_4^{2-} in every layers change much less when comparing with low-level cloud. SO_4^{2-} increases the radiative heating rates by about 0.01°C / d in cloudy layers. It causes the radiative heating rates to decrease a little in January, and increase in July. But the range of variation is within 0.01°C / d (See Table 2).

When there are high clouds SO_4^{2-} causes the solar radiation flux which arrives the surface to reduce by about 0.76 Wm^{-2} and 1.15 Wm^{-2}, respectively in January and July. The

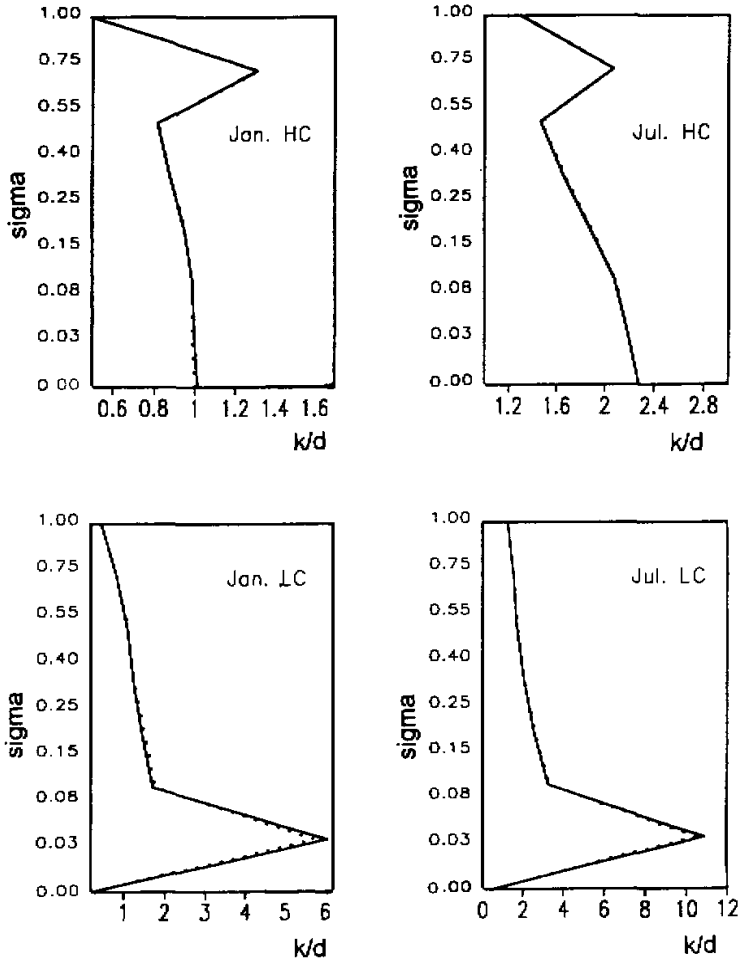

Fig. 6. The vertical profile of the solar radiative heating rate of SO_4^{2-} in cloudy atmosphere. Solid line: no SO_4^{2-}, dashed line: SO_4^{2-} included (unit: °C / d) HC: high cloud LC: low cloud.

variation is less than that in clear sky. The solar radiation flux absorbed by earth-atmosphere system has decrease of about 0.55 Wm^{-2} in January and 0.46 Wm^{-2} in July. It is much larger than that with low-level cloud, but close to the value in clear sky.

It is shown that the existence of cloud can change the pattern of radiative forcing of SO_4^{2-} remarkably, and there are significant differences between the effects of high-level cloud and low-level cloud, and their effects are not only manifested in the cloudy layer, but also in the layers below and above the cloudy layer. The effects of the low-level cloud with relatively large optical thickness are especially obvious. Above analyzed results are based on the given cloud types, height, thickness and other optical characteristics. We further did some experiments to investigate and compare the atmospheric radiative forcing effects of the different cloud types, optical thickness, and cloudy layers. The results show that the radiative effects of SO_4^{2-} in the cloudy atmosphere changes very significantly with the optical features of clouds.

V. CONCLUSION AND DISCUSSION

From numerical simulations and radiation transfer calculation, the following conclusions can be drawn:

(1) In East Asia, SO_4^{2-} concentration has obvious regional distribution characters, with its high value areas locating in Southwest China, the middle and lower reaches of the Yangtze River and lower reaches of the Yellow River in China. The averaged content in East Asia is much higher than the average in the Northern Hemisphere. Anthropogenic SO_4^{2-} mainly distributes in low layer of the troposphere below 2 km.

(2) Being affected by precipitation and wind fields, the concentration of SO_4^{2-} is largest in October, then successively in January, April and July, thus being of very significant seasonal variation.

(3) Under clear sky the reflection effects of SO_4^{2-} significantly decrease the solar radiation flux which arrives the surface. It also abates the solar radiation absorbed by the earth-atmosphere system and causes the cooling of atmosphere. But the solar radiative heating rate in the atmosphere increases a little perhaps due to the change of optical thickness resulting from the scattering of SO_4^{2-}. The spatial and temporal distributions of the radiative effects of SO_4^{2-} are mainly determined by the spatial and temporal distributions of its concentration.

(4) Both the high and the low cloud can influence the effects of SO_4^{2-} on the solar radiation flux absorbed by the earth-atmosphere and the radiative heating rate in every layer, especially in cloudy layer. The effects of SO_4^{2-} are related to the types, height, optical depth and other optical characteristics of clouds.

This paper only gives some very preliminary results on the radiative effects of SO_4^{2-} under the specific atmospheric conditions. To know more about the effects of SO_4^{2-} on climatic change, it is necessary to do more numerical simulations using general circulation model or regional climate model. Only direct radiative forcing of SO_4^{2-} is incorporated in the radiation transfer calculation. In fact, as one kind of cloud condensation nuclei, the change of SO_4^{2-} content would influence the optical characteristics and lifetime of cloud and precipita-

tion, then change the radiative forcing and climate fields. It is so called indirect forcing of SO_4^{2-}. This indirect forcing is very significant comparing with its direct forcing, though the uncertainty it causes is still very large.

In addition, to a certain degree we found the consistency between the variation of temperature in China since 1980s and the radiative effects of SO_4^{2-} according to the annual averaged climatic observed data(Qian et al.,1996), but further analysis results show that, since 1980s, most areas over South China have been cooling, especially during daytime; further-more, the mean temperature in summer decreased more than that in winter. However, the calculated results in this work show that the SO_4^{2-} concentration in January is larger than that in July, so are the albedo effects and radiative forcing. Therefore, to understand the climatic change that we have observed is a much more difficult and complicated task than the one we anticipate at present.

REFERENCES

Akimoto Hajime (1994), Distribution of SO_2, NO_x and CO_2 emissions from fuel combustion and industrial activities in Asia with $1° \times 1°$ resolution, *Atmospheric Environment*, **28:** 213-225.

Charlson, R. J., et al.(1991a), Perturbation of the Northern Hemisphere Radiative balance by backscattering from anthropogenic sulfate aerosols, *Tellus*, **43AB:** 152-163.

Charlson R. J., J. Langner (1991b), Sulphate aerosol and climate, *Nature*, **348:** 22.

Charlson R. J., S. E. Schwartz, J. M. Hales et al. (1992), Climate forcing by anthropogenic aerosols, *Science*, **255:** 423-430.

Danny Harvey L. D. (1995), Warm days, hot nights, *Nature*, **377:** 15-16.

Huang, M. Y., D. Y. He, Z. F. Wang (1996), Modelling studies on sulfur deposition and transport in East Asia, *Water Soil and Pollution*, **85:** 1921-1926.

IPCC (1994), Radiative forcing of climate change, The 1994 report of the scientific assessment working group of IPCC, Cambridge University Press.

Kneizys F. X., E. P. Shettle (1988), AFGL-TR-88-0177.

Matthews E.(1983), Global vegetation and land use: New high-resolution data bases for climate studies, *J. Climate and Applied Meteorology*, **22:** 474-487.

Qian, Y., C. B. Fu et al.(1996), Effects of Industrial SO_2 Emission on the Temperature Variation Over China and East Asia, *Research on Climate and Environment*, **1(2):** 143-149.

Qian, Y., C. B. Fu(1997), SO_2 emission, sulfate aerosol and climate change, *Advance in Earth Sciences*, **12(5):** 440-446.

Stamnes, K, Tsay S-Chee, W. Wiscombe(1988), Numerically stable algorithm for discrete- ordinate method radiation transfer in multiple scattering and emitting layered media, *Appl. Opt.*, **27:** 2502-2509.

WCP-55, Deepak, A and H. E. Gerber(1983), Report on export meeting on aerosols and their climates, WMO, 103.